ESANN 2025 proceedings, European Symposium on Artificial Neural Networks, Computational Intelligence and Machine Learning. Bruges (Belgium) and online event, 23-25 April 2025, i6doc.com publ., ISBN 9782875870933. Available from http://www.i6doc.com/en/.

Inferring Underwater Topography with Finite Volume Neural Networks

Coşku Can Horuz,[2] Matthias Karlbauer,[1] Timothy Praditia,[3]
Sergey Oladyshkin,[3] Wolfgang Nowak,[3] and Sebastian Otte[2]

1 – Neuro-Cognitive Modeling, University of Tübingen,
2 – Adaptive AI Lab, Institute of Robotics and Cognitive Systems,
University of Lübeck,
3 – Department of Stochastic Simulation and Safety Research for Hydrosystems,
University of Stuttgart.

Abstract. Partial differential equations (PDEs) find applications across various scientific and engineering fields. There is a growing trend for integrating physics-aware machine learning models to solve PDEs. Among them, the Finite Volume Neural Network (FINN) has proven to be efficient in uncovering latent structures in data. This study explores the capabilities of FINN in the investigation of shallow-water equations, which simulate wave dynamics in coastal regions. Specifically, we investigate the efficacy of FINN in reconstructing underwater topography. We find that FINN excels at inferring topography solely from wave dynamics, stressing the importance of application-specific inductive bias in neural network architectures.

1 Introduction

Machine learning models that incorporate physical principles follow the governing rules of the problem at hand. Physics-aware models are reported to be superior to pure ML models when simulating physical processes [1, 2]. However, various physics-aware models lack the ability to explicitly incorporate physical equations. The recently introduced finite volume neural network (FINN) marks a significant step forward in addressing this limitation [3, 4, 5]. FINN combines partial differential equations (PDEs) with the learning capabilities of artificial neural networks and models spatiotemporal dynamics in a mathematically compositional manner. A notable feature of FINN is its ability to directly incorporate boundary conditions (BCs) in order to explicitly enforce the physical structure in the model [4]. As a result, FINN generalizes well beyond the BC values encountered during training and infers unknown BCs to reveal the hidden structure in the data [6, 7].

In this study, we expose FINN to a new set of PDEs, called shallow-water equations (SWEs) that model the wave dynamics in coastal regions. We further study the capability of FINN in reconstructing the topography depending on the waves at the surface. We adapt FINN's architecture to SWE and by doing so, open a new pathway for broader applications of FINN. We compare the quality of the inferred topography with two models, DISTANA [8] and PhyDNet [9]. Our results indicate that all models are able to model the physical processes and predict the wave patterns. Yet, FINN's induced physical structure bias results

ESANN 2025 proceedings, European Symposium on Artificial Neural Networks, Computational Intelligence and Machine Learning. Bruges (Belgium) and online event, 23-25 April 2025, i6doc.com publ., ISBN 9782875870933. Available from http://www.i6doc.com/en/.

in smaller modeling errors and a higher accuracy in reconstructing the hidden topography. Our code repository can be found under this link.

2 Data and Methods

SWEs represent fluid dynamics, where the wavelength λ (distance between consecutive waves) is much larger than the depth of the fluid H, i.e., $\frac{H}{\lambda} \ll 1$ (shallow water assumption). As a simplified version of the Navier-Stokes equations, SWEs find most applications in aquatic environments, although the corresponding fluid does not necessarily have to be water. The specific form of the SWEs employed in this study are taken from [10] and defined as follows:

$$\frac{\partial \eta}{\partial t} + \frac{\partial}{\partial x}[u(H+\eta)] + \frac{\partial}{\partial y}[v(H+\eta)] = 0, \tag{1}$$

$$\frac{\partial u}{\partial t} = -g\frac{\partial \eta}{\partial x}, \tag{2}$$

$$\frac{\partial v}{\partial t} = -g\frac{\partial \eta}{\partial y}, \tag{3}$$

where u and v are the velocity vectors in x- and y-directions, respectively. H is the topography of the fluid representing the depth of each grid cell in meters. η is the displacement of the free surface, essentially capturing the vertical deviation of the fluid surface from the mean depth as waves propagate. Lastly, t denotes time and g expresses the gravitational force.

2.1 Models

This section provides an overview of the models under comparison: PhyDNet, DISTANA, and FINN. The descriptions of PhyDNet and DISTANA are presented in less detail in comparison to FINN, as the model of interest.

PhyDNet PhyDNet is a physics-aware encoder-decoder model introduced in [9]. After encoding the input at time step t, the information is disentangled into two separate networks: PhyCell and ConvLSTM-Cell. Inspired by physics, PhyCell implements spatial derivatives up to a desired order and can approximate solutions of a wide range of PDEs, e.g., the heat equation, wave equation, and the advection-diffusion equation. ConvLSTM-Cell is incorporated to *learn* the spatiotemporal processes, resulting in a hybrid model.

DISTANA The distributed spatiotemporal graph artificial neural network architecture (DISTANA) is a hidden state inference model for time series prediction. It encodes two different kernels in a graph structure. First, the *prediction kernel* (PK) network predicts the dynamics at each spatial position while being applied to each node of the underlying mesh. Second, the *transition kernel* (TK) network coordinates the lateral information flow between PKs. Due to the regular grid structure of the data in this work, we implement linear mappings as TKs, as done in the original work [8].

ESANN 2025 proceedings, European Symposium on Artificial Neural Networks, Computational Intelligence and Machine Learning. Bruges (Belgium) and online event, 23-25 April 2025, i6doc.com publ., ISBN 9782875870933. Available from http://www.i6doc.com/en/.

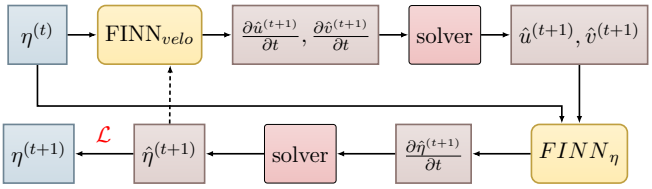

Fig. 1: Modified process chain implementation of FINN. Dark black arrows show the forward pass. The prediction is fed back into the model autoregressively as closed-loop predictions (dashed arrow).

FINN The finite volume neural network, introduced in [4, 3] represents a novel fusion of the finite volume method (FVM), a numerical discretization technique in computational physics, with the learning capabilities of neural networks. The FVM spatially discretizes continuous PDEs by transforming them into algebraic (linear) equations defined over a finite number of control volumes. These control volumes possess distinct states and exchange fluxes according to the conservation law. By embedding FVM principles into FINN, the model is inherently constrained to enforce (partially) known laws from physics to excel in interpretability, generalization, and robustness. Originally, FINN was designed to solve non-linear spatiotemporal advection-diffusion-reaction processes, formulated in [4] as

$$\frac{\partial u}{\partial t} = D(u)\frac{\partial^2 u}{\partial x^2} - v(u)\frac{\partial u}{\partial x} + q(u), \tag{4}$$

where u encodes a state as a function of time t and spatial coordinate x. D is the diffusion coefficient, which manages the equilibration between high and low concentrations, v is the advection velocity, which represents the movement of concentration due to the bulk motion of a fluid, and q is the source/sink term, which increases or decreases the quantity of u locally.

In order to model spatiotemporal wave dynamics, we reformulate FINN such that its structure resembles the SWE. Concretely, we employ a two-stage process, first solving for velocities u and v by means of which η is solved subsequently.[1] The resulting process chain is outlined in Figure 1. Each FINN module implements an adequately tailored FINN architecture to approximate the different components of SWE, i.e., u, v, and η.

In order to expose the models to a diverse range of topographies, we trained the models on different H grids (see left plot in Figure 2 for an example), where H is rotated with a random angle $\phi \in [0, 2\pi]$ and the depth of H is scaled with a random number $\beta \in [0.5, 1.0]$ such that the average depth is between $50-100m$ in each sample. After training, we challenge models to infer a bumpy and more non-linear topography (see right plot in Figure 2) by setting H as learnable parameter. To enforce the inference of a continuous surface, a smoothness-constraint λ

[1] We employ the Euler solver here, although more sophisticated solvers can also be implemented. In our case, however, more advanced solvers did not improve the results.

ESANN 2025 proceedings, European Symposium on Artificial Neural Networks, Computational Intelligence and Machine Learning. Bruges (Belgium) and online event, 23-25 April 2025, i6doc.com publ., ISBN 9782875870933. Available from http://www.i6doc.com/en/.

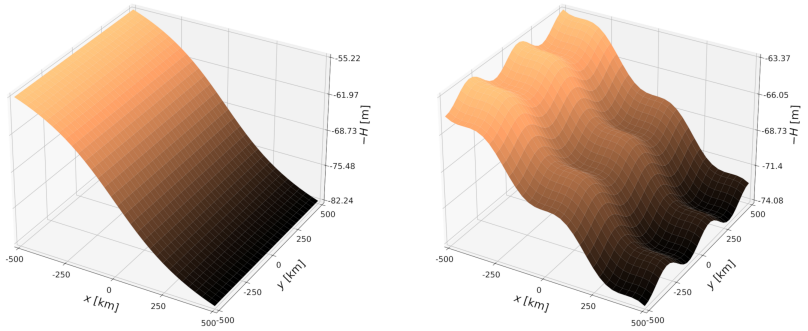

(a) Train (b) Inference

Fig. 2: Topography of the training and inference set. The training topography (left) is smooth and exhibits a larger depth range. The inference topography (right) is more non-linear and bumpy. The depth scale for the particular topography was randomly chosen as $\beta = 0.68$.

(set to 5×10^{-3} for PhyDNet and 5×10^{-7} for the others) was introduced, penalizing significant deviations between adjacent cells. Furthermore, to facilitate the inference of H at the boundaries where the velocity vectors are zero (no-slip condition), we introduce another regularization term, $\lambda_{edge} = 5 \times 10^{-7}$ to push the inferred H towards the values sitting well in the simulation domain. The use of λ_{edge} improved the performance across all models, albeit both PhyDNet and DISTANA still struggled to produce accurate reconstructions along the edges.

3 Results

Throughout all experiments, the primary objective is to reconstruct the topography with high accuracy. Main results are reported in Table 1. While all three models successfully learn the SWEs and accurately predict subsequent wave states with varying levels of accuracy, DISTANA and FINN outperform PhyDNet in reconstructing the topography. The inference error exhibited by PhyDNet can be attributed to the application of a stricter grid regularizer aimed at en-

Table 1: Reconstruction errors per model. Test error relates to deficits in predicting the shallow water dynamics under use of the inferred topography.

Model (params)	DISTANA (19k)	PhyDNet (185k)	FINN (230)
Train error	$(6.4\pm1.6)\times10^{-5}$	$(5.2\pm2.0)\times10^{-5}$	$1\times10^{-5}\pm6\times10^{-9}$
Test error	$(5.0\pm1.1)\times10^{-5}$	$(5.9\pm4.4)\times10^{-5}$	$(2.7\pm0.1)\times10^{-6}$
Full rec. error	0.913 ± 0.125	10.71 ± 5.906	0.262 ± 0.013
Inner rec. error	0.516 ± 0.121	10.33 ± 6.160	0.237 ± 0.018

ESANN 2025 proceedings, European Symposium on Artificial Neural Networks, Computational Intelligence and Machine Learning. Bruges (Belgium) and online event, 23-25 April 2025, i6doc.com publ., ISBN 9782875870933. Available from http://www.i6doc.com/en/.

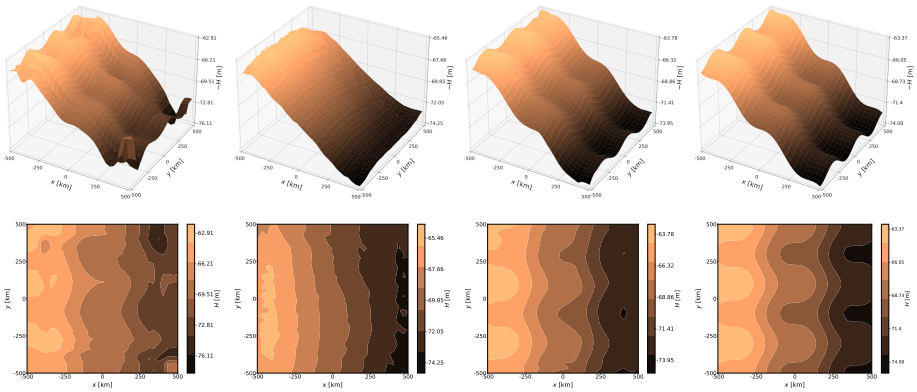

(a) DISTANA (b) PhyDNet (c) FINN (d) Data

Fig. 3: Examples of inferred topography fields per model in 3D (top) and as a top-view contour plot (bottom).

hancing the reconstruction quality. However, when applying the same λ value for PhyDNet as used in DISTANA and FINN, the reconstruction error triples and the inferred topographies exhibit large spikes. We depict the most accurate topography reconstructions of each model in Figure 3, which confirm that FINN and DISTANA manage to reconstruct the topography with FINN scoring superior. In particular, DISTANA exhibits notable deviations along the edges, which we attribute to an inadequate representation of the boundary condition. In contrast, FINN applies boundary conditions rigorously based on the governing equations, whereas DISTANA and PhyDNet rely on convolution operations for this purpose, leading to poorer edge reconstruction. To reduce boundary effects, we also present inference errors in Table 1, calculated within a central 28×28 subregion extracted from the original 32×32 field. While the error difference between DISTANA and FINN is closer within the inner domain, DISTANA's error still remains twice as large compared to FINN. PhyDNet, on the contrary, fails to produce meaningful topography reconstructions, which is also reflected in the high standard deviations.

4 Discussion

We assessed the capabilities of DISTANA, PhyDNet, and FINN at inferring underwater topography, which parameterizes the shallow water equations. FINN was modified to characterize a system of three coupled PDEs. Essentially, we implemented a two-staged process combining two separate FINN modules to subsequently generate a prediction for the SWEs velocity vectors u and v, which give rise to approximating the actual wave depth η.

Along with the lowest test error, the resulting FINN model produced accurate reconstruction of the underwater topography. DISTANA managed to solve

ESANN 2025 proceedings, European Symposium on Artificial Neural Networks, Computational Intelligence and Machine Learning. Bruges (Belgium) and online event, 23-25 April 2025, i6doc.com publ., ISBN 9782875870933. Available from http://www.i6doc.com/en/.

the SWE system and inferred the underlying topographical structure reasonably well, which aligns with findings from a previous study [11], where DISTANA inferred a latent land-sea mask. PhyDNet, despite its physics-aware formulation, managed to model the SWE but struggled in the generalization task to reconstruct a different topography.

In conclusion, this study suggests implementing the physical structures into deep learning models, encapsulating application-specific inductive bias to complement the learning abilities of neural networks. Furthermore, given that SWE represents a simplified version of Navier-Stokes equations, further research efforts could be directed towards integrating more complex versions of these equations into FINN's framework.

References

[1] George Em Karniadakis, Ioannis G Kevrekidis, Lu Lu, Paris Perdikaris, Sifan Wang, and Liu Yang. Physics-informed machine learning. *Nature Reviews Physics*, 3(6):422–440, 2021.

[2] Maziar Raissi, Paris Perdikaris, and George E Karniadakis. Physics-informed neural networks: A deep learning framework for solving forward and inverse problems involving nonlinear partial differential equations. *Journal of Computational physics*, 378:686–707, 2019.

[3] Timothy Praditia, Matthias Karlbauer, Sebastian Otte, Sergey Oladyshkin, Martin V. Butz, and Wolfgang Nowak. Finite volume neural network: Modeling subsurface contaminant transport. In *International Conference on Learning Representations (ICRL) – Workshop Deep Learning for Simulation*, 2021.

[4] Matthias Karlbauer, Timothy Praditia, Sebastian Otte, Sergey Oladyshkin, Wolfgang Nowak, and Martin V. Butz. Composing partial differential equations with physics-aware neural networks. In *International Conference on Machine Learning (ICML)*, 2022.

[5] Timothy Praditia, Matthias Karlbauer, Sebastian Otte, Sergey Oladyshkin, Martin V Butz, and Wolfgang Nowak. Learning groundwater contaminant diffusion-sorption processes with a finite volume neural network. *Water Resources Research*, 2022.

[6] Coşku Can Horuz, Matthias Karlbauer, Timothy Praditia, Martin V. Butz, Sergey Oladyshkin, Wolfgang Nowak, and Sebastian Otte. Inferring boundary conditions in finite volume neural networks. In *International Conference on Artificial Neural Networks (ICANN)*, pages 538–549. Springer Nature Switzerland, 2022.

[7] Coşku Can Horuz, Matthias Karlbauer, Timothy Praditia, Martin V. Butz, Sergey Oladyshkin, Wolfgang Nowak, and Sebastian Otte. Physical domain reconstruction with finite volume neural networks. *Applied Artificial Intelligence*, 37(1):2204261, 2023.

[8] Matthias Karlbauer, Sebastian Otte, Hendrik P.A. Lensch, Thomas Scholten, Volker Wulfmeyer, and Martin V. Butz. A distributed neural network architecture for robust non-linear spatio-temporal prediction. In *28th European Symposium on Artificial Neural Networks (ESANN)*, pages 303–308, Bruges, Belgium, October 2020.

[9] Vincent Le Guen and Nicolas Thome. Disentangling physical dynamics from unknown factors for unsupervised video prediction. In *Proceedings of the IEEE/CVF Conference on Computer Vision and Pattern Recognition*, pages 11474–11484, 2020.

[10] Pijush K. Kundu and Ira M. Cohen. *Fluid Mechanics*. Elsevier Academic Press, California, USA, third edition, 2004.

[11] Matthias Karlbauer, Tobias Menge, Sebastian Otte, Hendrik P. A. Lensch, Thomas Scholten, Volker Wulfmeyer, and Martin V. Butz. Latent state inference in a spatiotemporal generative model. In *International Conference on Artificial Neural Networks (ICANN)*, pages 384–395. Springer International Publishing, 2021.